# Inelastic transport detection of spin quantum tunneling and spin relaxation in single-molecule magnets in the absence of a magnetic field

Rui-Qiang Wang, R. Shen, Shi-Liang Zhu, Baigeng Wang, and D. Y. Xing

# Inelastic transport detection of spin quantum tunneling and spin relaxation in the absence of a magnetic field

Rui-Qiang Wang[1], R. Shen[2], Shi-Liang Zhu[1], Baigeng Wang[2], and D.Y. Xing[2]

[1] *Laboratory of Quantum Information Technology, ICMP and SPTE,*
*South China Normal University, Guangzhou 510006, China*

[2] *National Laboratory of Solid State Microstructures and Department of Physics, Nanjing University, Nanjing 210093, China*

(Dated: March 30, 2012)

In a scanning tunneling microscope configuration (STM), we study theoretically the effects of quantum tunneling of magnetization (QTM) as well as transport-induced spin relaxation on the electron transport through a single-molecule magnet deposited on a metallic surface. It is shown that for the STM with a high spin-polarized tip, the inelastic current is completely determined by the QTM channel at low temperatures and by the spin relaxation channel at higher temperatures, from which the tunnel splitting and spin-relaxation rate can be directly determined in despite of the absence of a magnetic field. The two types of different mechanisms can be distinguished from each other by current and/or noise spectra.

## I. INTRODUCTION

Electronic transport through high-spin nanomagnets, such as $Mn_{12}$ and $Fe_8$, constituting the basis of molecular spintronics, has become an intense topic of study[1–4] for fundamental physics and potential application in magnetic data storage or quantum computing. Owing to its high spin and large magnetic easy-axis anisotropy, the nanomagnet forms a ladder-shaped structure of magnetic levels. These magnetic features can be preserved and even electrically controllable in a single-molecule-transistor geometry[5–7], in which the signatures of magnetic states and magnetic anisotropy can be identified.

The nanomagnet structures combine the classical properties of magnets with the intrinsic quantum nature. Their most outstanding feature is quantum tunneling of magnetization (QTM), a macroscopic quantum effect resulting from the intrinsic transverse anisotropy. The QTM induces the spin resonant tunneling by mixing pairs of degenerated magnetic states with opposite spins, separated by a strong anisotropy barrier. The powerfully experimental evidences for supporting the QTM are the characteristic steps in hysteresis loops and the interference effect of Berry's phase on the magnetization at temperature below 1K while the external field is applied to single-molecule magnets (SMMs)[8–10]. Recently, probing of the QTM fingerprint on the electronic transport has attracted great interest. The quantum-tunneling-induced Kondo effect in the SMMs, based on a joint effect of itinerant electrons and the QTM, was theoretically predicted[11,12]. Experimentally, great efforts[13,14] have been made along this line, even though there still remains a challenge to it. The spin tunneling was also predicted to be determined by the identification of the fake resonances in current and noise spectroscopy[15]. Recently, an interesting project to detect the QTM was the observation of the Berry-phase blockade of the stationary current in the sequential tunneling for the SMM placed between oppositely spin-polarized source and drain leads[16].

Technologic breakthroughs have permitted to locally probe the magnetic anisotropy of a single SMM or atom adsorbed on metallic surfaces[17–20] by using a scanning tunneling microscopy (STM). Nevertheless, how to extract the QTM fingerprint directly in electron transport spectroscopy still remains a great challenge. Placing the STM tip above one SMM, G.-H. Kim and T.-S. Kim[21] studied the inelastic electron tunnel spectroscopy, and found that the QTM can lead to a stepwise increase in the linear response conductance if a longitudinal magnetic field is applied, and the conductance at each step oscillates as a function of additional transverse magnetic field. It is an interesting idea to get rid of the external magnetic field and still get a fingerprint of the QTM effect. Our proposal is that such an object can be realized by employing a spin-polarized STM[22–24], which was recently applied to provide direct visualization of stationary spin states and spin dynamics in nanomagnets. With the interplay of spin-polarized conducting electrons and the localized molecule magnet, the spin-polarized STM was used to explore the spin-transfer torque of molecular magnitizations[25–28].

In this paper, we apply the spin-polarized STM model to study theoretically the inelastic tunneling spectroscopy of SMMs deposited on a metallic substrate. In this spin-polarized transport, an exotic spin relaxation mechanism for the local spin is inevitably introduced. It originates from the exchanged interaction with electrons of spin-flip tunneling out of and back into the same lead. It can be ignored for normal leads because of the cancelation of the contributions from spin-up and -down electrons, but it plays a role for magnetized leads[25,29,30]. An important issue is how to evaluate this transport-induced relaxation rate since it only indirectly influences the current by changing

of the magnetic occupation. In our study, it is found that the QTM effect of the SMM can be probed from the stationary inelastic current by use of the STM with a high-polarized tip. At low temperatures the tunnel splitting completely determines the magnitude of the inelastic current, favorable to the observation of the QTM effect. At higher temperatures the spin-relaxation channels govern the inelastic current as a new transport mechanism, which can be used to detect the spin relaxation rate. The rest of the paper is organized as follows. In Sec. II the theoretical model is provided for calculations of the tunneling current, and in Sec. III the inelastic current and shot noise are discussed in detail. A short summary is given in the last section.

## II. MODEL AND METHOD

Consider a single SMM deposited on a normal metallic substrate and a magnetic STM tip is placed right above the SMM[17,21]. The system Hamiltonian can be written as $H = H_{tip} + H_{sub} + H_{SMM} + H_T$, where the first three terms describe the tip, substrate, and SMM as decoupled systems, whereas the last term (tunneling Hamiltonian) introduces interactions between them. With notation $\eta = t(s)$ for the tip (substrate), we write $H_{tip} + H_{sub} = \sum_{\eta k \sigma} \varepsilon_{\eta k \sigma} c^\dagger_{\eta k \sigma} c_{\eta k \sigma}$ where $c^\dagger_{\eta k \sigma}$ ($c_{\eta k \sigma}$) is the creation (annihilation) operator of electrons with spin $\sigma$, wave vector $k$, and the energy dispersion $\varepsilon_{\eta k \uparrow(\downarrow)} = \varepsilon_{\eta k} \pm h_\eta$ with the exchange field $h_t = h$ for the magnetic tip and $h_s = 0$ for the metallic substrate. The tunneling Hamiltonian is given by[25,29]

$$H_T = \sum_{\eta\eta',kk',\sigma\sigma'} (J_{\eta\eta'} c^\dagger_{\eta k \sigma} \frac{\tau_{\sigma\sigma'} \cdot \mathbf{S}}{2} c_{\eta'k'\sigma'} + \frac{J_d}{2} c^\dagger_{\eta k \sigma} c_{\eta'k'\sigma}) \tag{1}$$

where $J_{\eta\eta'}$ characterizes the Kondo-like exchange coupling between the local spin $\mathbf{S} = (S_x, S_y, S_z)$ of the SMM and transport electrons while $J_d$ features the coupling of the direct tunneling between the tip and substrate. The magnetic easy-axis of the SMM is chosen along the $z$ direction parallel to the tip magnetization, and $\tau = (\tau^x, \tau^y, \tau^z)$ denotes the Pauli spin operator for the transport electrons. This tunneling model describes essentially deep cotunneling, in which the orbit levels are out of resonance with the Fermi level and thereby the sequential tunneling is exponentially suppressed.

The spin Hamiltonian of the SMM is

$$H_{SMM} = -DS_z^2 - \sum_{n=1,2} \frac{B_{2n}}{2}(S_+^{2n} + S_-^{2n}). \tag{2}$$

In general, the longitudinal magnetic anisotropy $D$ dominates over the second-order and fourth-order transverse anisotropy $B_{2n}$. In the absence of the transverse term, a ladder-shaped level spectra are constructed, $\varepsilon_m = -Dm^2$ with $m = 0, \pm 1, ... \pm S$ as the magnetic quantum number, forming degenerated states $|\pm m\rangle$ located separately in two magnetic wells with opposite spin projection. As a perturbation, turning on the weak transverse anisotropy $B_{2n}$ terms leads to mixing of the degenerated states $|\pm m\rangle$ via $S_\pm = S_x \pm iS_y$, and lifts the corresponding degenerated levels by a tunnel splitting $\Delta_{m,-m}$, often referred to as the QTM effect. To obtain analytical formula, we introduce the two-level Landau-Zener model as done in Refs.[21,31]. By projecting $H_{SMM}$ in Eq. (2) onto a two-state subsystem $\{|m\rangle, |-m\rangle\}$, it can be replaced with an effective Hamiltonian

$$\tilde{H}_{SMM} = \begin{bmatrix} \varepsilon_m & \Delta_{m,-m}/2 \\ \Delta_{m,-m}/2 & \varepsilon_{-m} \end{bmatrix}. \tag{3}$$

This description is valid as long as $\Delta_{m,-m}$ is much smaller than level spacing $|\varepsilon_{mm'}| = |\varepsilon_m - \varepsilon_{m'}|$, which is usually satisfied due to the fact of $B_{2n} \ll D$.

Under the Born and Markov approximations, the generalized master equations that describe the dynamical evolution of density matrix elements ($\rho_m = \langle m | \rho | m \rangle$ and $\rho_{mm'} = \langle m | \rho | m' \rangle$) for the SMM can be obtained as[31,32]

$$\dot{\rho}_m = \frac{i\Delta_{m,-m}}{2\hbar}(\rho_{m,-m} - \rho_{-m,m}) + \sum_{\eta\eta',m'\neq m} (W^{\eta\leftarrow\eta'}_{m,m'} \rho_{m'} - W^{\eta'\leftarrow\eta}_{m',m} \rho_m), \tag{4}$$

$$\dot{\rho}_{m,-m} = -\frac{1}{2} \sum_{\eta\eta' l} (W^{\eta\leftarrow\eta'}_{l,m} + W^{\eta\leftarrow\eta'}_{l,-m}) \rho_{m,-m} + \frac{i\Delta_{m,-m}}{2\hbar}(\rho_m - \rho_{-m}). \tag{5}$$

Here the diagonal element $\rho_m$ stands for the probability of finding the magnetic state in $|m\rangle$. $W^{\eta'\leftarrow\eta}_{m',m}$ is the transition rate of transport electrons going from lead $\eta$ to $\eta'$, accompanied with the SMM spin quantum number changing

from $m$ to $m'$, whose evaluating formula will be given in Eqs. (8) and (9). In the incoherent tunneling case of the time longer than the decoherence time of off-diagonal elements $\rho_{m,-m}$, their time dependence can be neglected, i.e., $\dot{\rho}_{m,-m} = 0$,[31,32] so that Eq. (3) is reduced to be

$$\dot{\rho}_m = \sum_{\eta\eta',m'\neq m} (W^{\eta\leftarrow\eta'}_{m,m'} + \delta_{m,-m'}\Gamma_{m,m'})\rho_{m'} - (W^{\eta'\leftarrow\eta}_{m',m} + \delta_{m',-m}\Gamma_{m',m})\rho_m, \tag{6}$$

where $\Gamma_{m,m'} = \Delta^2_{m,m'}/\sum_{\eta\eta'l}\hbar^2(W^{\eta\leftarrow\eta'}_{l,m} + W^{\eta\leftarrow\eta'}_{l,m'})$ describes the QTM-related tunneling rate between states $|m\rangle$ and $|m'\rangle$. When the bias voltage is applied between the STM tip and the metallic substrate, the stationary electronic current which flows through the SMM is given by

$$I = -e\sum_{m',m} \rho_{m'}(W^{s\leftarrow t}_{m,m'} - W^{t\leftarrow s}_{m,m'}). \tag{7}$$

We wish to point out here that the tunneling rate $\Gamma_{m,m'}$ does not manifest in Eq. (7), but has contribution to the current via the change of $\rho_m$. The transition rate is evaluated by use of the Fermi's Golden rule, yielding $W^{\eta'\leftarrow\eta}_{m',m} = W^{(el)\eta'\leftarrow\eta}_{m',m} + W^{(in)\eta'\leftarrow\eta}_{m',m}$, with

$$W^{(el)\eta'\leftarrow\eta}_{m',m} = \frac{\pi}{2\hbar}\delta_{mm'}\left[(J_d + mJ_{\eta\eta'})^2 D^\eta_\uparrow D^{\eta'}_\uparrow + (J_d - mJ_{\eta\eta'})^2 D^\eta_\downarrow D^{\eta'}_\downarrow\right] F(\mu_\eta - \mu_{\eta'}), \tag{8}$$

$$W^{(in)\eta'\leftarrow\eta}_{m',m} = \frac{\pi}{2\hbar}J^2_{\eta\eta'}\left[\left|S^{m',m}_+\right|^2 D^\eta_\uparrow D^{\eta'}_\downarrow + \left|S^{m',m}_-\right|^2 D^\eta_\downarrow D^{\eta'}_\uparrow\right] F(\varepsilon_{mm'} + \mu_\eta - \mu_{\eta'}). \tag{9}$$

Here $W^{(el)\eta'\leftarrow\eta}_{m',m}$ is the transition rate for the elastic tunneling, including the direct and exchange tunneling with spin conversion as well as the interference between them, where $D^\eta_\sigma$ is the density of states of spin-$\sigma$ electron at the Fermi level, $F(\varepsilon) = \varepsilon/(1 - e^{-\varepsilon/k_B T})$ with $T$ as temperature and $\mu_\eta$ as the electrochemical potential at lead $\eta$. It directly contributes to the elastic current flow for $\eta' \neq \eta$, but does not affect $\rho_m$. $W^{(in)\eta'\leftarrow\eta}_{m',m}$ is the transition rate for the inelastic tunneling, involving not only the spin-flip electron tunneling of the different leads ($t \to s$ or $s \to t$), but also that of the same leads ($t \to t$ or $s \to s$) via spin excitation $S^{m',m}_+$ and spin disexcitation $S^{m',m}_-$ processes, where $S^{m',m}_\pm = [S(S+1) - m(m\pm1)]^{1/2}\delta_{m',m\pm1}$. $W^{(in)s\leftarrow t}_{m',m}$ and $W^{(in)t\leftarrow s}_{m',m}$ have contribution to both $\rho_m$ and the current. $\gamma_{m',m} = W^{(in)t\leftarrow t}_{m',m} + W^{(in)s\leftarrow s}_{m',m}$ is interpreted as the transport-induced spin relaxation for the SMM spin, stemming from the contributions of the electrons of spin-flip tunneling out of and back into the same lead. Similar to $\Gamma_{m,m'}$, it contributes to the current via the change of $\rho_m$.

## III. RESULTS AND DISCUSSION

In this section we perform numerical calculations of the current for synthesized material Ni$_4$[33] with local spin $S = 4$, $D = 1.33$K, $B_2 = -0.034$K, and $B_4 = 0.003$K. The tunnel splitting $\Delta_{m,-m}$ is obtained by exactly numerical diagonalization of $H_{SMM}$ in Eq. (2). Define the spin polarization of leads as $\chi_\eta = (D^\eta_\uparrow - D^\eta_\downarrow)/D^\eta_0$ with $D^\eta_0 = D^\eta_\uparrow + D^\eta_\downarrow$, and so for the nonmagnetic substrate $\chi_s = 0$. A large bias limit is considered, i.e., $eV = \mu_t - \mu_s$ is much greater than $\varepsilon_{mm'}$ and $k_B T$. In this case, $W^{t\leftarrow s}_{m,m'} \simeq 0$ can be neglected because of $F(-eV) \simeq 0$, and so the stationary inelastic current is given by $I_{in} = -e\sum_{m,m'\neq m} \rho_{m'}W_{m,m'}$. Here and henceforth $W^{(in)s\leftarrow t}_{m',m}$ has been relabeled as $W_{m,m'}$ for simplicity. In the steady state, $\rho_m$ can be obtained from Eq. (6) with $\dot{\rho}_m = 0$, which consists of $2m + 1$ linear equations, together with normalization condition $\sum_m \rho_m = 1$.

For nonmagnetic tip ($\chi_t = 0$), the stationary inelastic current is plotted in Fig. 1(a), where $I_{in}$ is independent of the value of $\Delta_{m,m'}$. To see this point clearer, we consider a simply case of $S = 1$, in which the analytical expression for $I_{in}$ is easily obtained as

$$I_{in} = e\frac{2(W_{0,1} + \gamma_{0,1})W_{1,0} + 2(W_{1,0} + \gamma_{1,0})W_{0,1}}{W_{0,1} + \gamma_{0,1} + 2(\gamma_{1,0} + W_{1,0})}, \tag{10}$$

where the symmetry property of $W_{m',m} = W_{-m',-m}$ have been used in consideration of $W_{m',m} \propto [S(S+1) - m^2]F[D(m'^2 - m^2) + eV]$ following from Eq. (9). Obviously, the current is not related to $\Delta_{m,m'}$ and thus it is impossible to observe the QTM effect in the case of unpolarized tip. Besides, although the spin relaxation rate $\gamma_{m',m}$

modifies the current value quantitatively, it is not requisite for generating $I_{in}$. When $\gamma_{m,m'} \ll W_{m,m'}$ is negligibly weak, Eq. (10) reduces to $\frac{1}{I_{in}} = \frac{1}{4e}(\frac{1}{W_{0,1}} + \frac{2}{W_{1,0}})$. In this case, the total resistance can be interpreted as two resistances in series with transition loops $|\pm 1\rangle \rightarrow |0\rangle \rightarrow |\pm 1\rangle$ in each subwell[16], as shown in Fig. 1(b).

To probe the QTM and the spin relaxation, we study the spin-polarized inelastic current with $\chi_t \simeq 1$. The corresponding current as a function of temperature is indicated by the solid line in Fig. 1(c). As $T$ is increased, the polarized $I_{in}$-$T$ curve exhibits first a current plateau, then a prominent dip, and finally increases rapidly. Such a temperature dependence of $I_{in}$ is attributed to the spin relaxation rate $\gamma_{m',m}$ via $\rho_m$, rather than $W_{m',m}$ because $W_{m',m} \propto F(eV)$ is independent of $T$ in the large bias limit. It follows from Eq. (9) that $\gamma_{m',m} \propto F(\varepsilon_{mm'})$, being independent of $T$ at low temperatures ($k_B T \ll \varepsilon_{mm'}$) and approximately proportional to $T$ at higher temperatures ($k_B T \gg \varepsilon_{mm'}$). In what follows we will discuss $I_{in}$ in three temperature ranges.

At low temperatures ($T < 1.2$K), the spin relaxation rate $\gamma_{m,m'} \ll W_{m,m'}$ can be negligible. The plateau value of the resulting current increases monotonously with $\Delta_{4,-4}$, and vanishes at $\Delta_{4,-4} = 0$, as shown in Figs. 1(c) and 2(a). This QTM dependence can be understood as follows. In the case of $\chi_t \simeq 1$, i.e., $D_\downarrow^t \simeq 0$, the transition rate of decreasing $m$ vanishes due to $W_{m-1,m} \propto \left| S_-^{m',m} \right|^2 D_\downarrow^t \simeq 0$. Once one spin-up electron passes inelastically through the SMM, it drives the magnetic state always increased from $|m\rangle$ to $|m+1\rangle$ by $W_{m+1,m}$. Without $\Delta_{4,-4}$, the SMM spin will be finally saturated at state $|4\rangle$, which in turn stops the inelastic electron tunneling via spin blockade effect, resulting to $I_{in} = 0$. The finite QTM provides a channel of decreasing $m$ and so maintains the inelastic tunneling. For $S = 1$, we obtain $\rho_{-1} = W_{1,0}\Gamma_{-1,1}/C$, $\rho_0 = W_{0,-1}\Gamma_{-1,1}/C$, and $\rho_1 = W_{1,0}(W_{0,-1} + \Gamma_{-1,1})/C$ with normalization constant $C = W_{0,-1}W_{1,0} + W_{0,-1}\Gamma_{-1,1} + W_{1,0}\Gamma_{-1,1}$, and the current as

$$\frac{1}{I_{in}} = \frac{1}{2e}\left(\frac{1}{\Gamma_{-1,1}} + \frac{2}{W_{0,-1}} + \frac{1}{W_{1,0}}\right). \tag{11}$$

This clearly shows that if $\Gamma_{-1,1} \propto \Delta_{-1,1}^2 = 0$, the SMM spin will occupy the state $|1\rangle$ with $\rho_1 = 1$ and thus $I_{in}$ vanishes. Eq. (11) can be interpreted as three resistances in series with a transition loop $|1\rangle \rightarrow |-1\rangle \rightarrow |0\rangle \rightarrow |1\rangle$, as depicted in Fig. 2(b). From $\Gamma_{m,-m} \ll W_{m+1,m}$, it then follows that the QTM tunneling rate becomes a bottleneck of generating the current at low temperatures. Therefore, we can directly probe the QTM by the measurement of the inelastic current in this geometry. The present discussion is somewhat similar to that made by González and Leuenberger[16], who proposed the detection of the QTM in sequential tunneling through an SMM placed between two oppositely spin-polarized leads. In the present work, the probing of the QTM effect can be accessible in the STM system with only one spin-polarized tip, which might relax technological conditions and be more favorable to experimental observations. At this low temperature region, the magnetic parameters $D$ and $B_{2n}$ affect the current via the splitting-related rate $\Gamma_{-m,m}$. In Fig. 1(c), the width of current plateau is determined mainly by the longitudinal magnetic anisotropy $D$, which describes the energy barrier to overcome in spin reversal of the SMM, while the magnitude of current plateau is determined mainly by the transverse anisotropy $B_{2n}$, which is the ability to mix degenerated doublets $|\pm m\rangle$. Large anisotropy $D$ can widen the current plateau but meanwhile reduce its value to some extent. Strong enough anisotropy $B_{2n}$ is desirable because it can generate a large tunnel splitting $\Delta_{m,-m}$ and a pronounced current signature. In addition, when the tunnel splitting is tuned by an applied magnetic field[16], we also can observe the Berry-phase blockade since if $\Delta_{m,-m} = 0$, $I_{in}$ will be completely suppressed due to $\Gamma_{m,-m} \propto \Delta_{m,-m}^2$.

At higher temperatures ($T > 3.5$K), the current magnitude no longer depends on $\Delta_{m,-m}$ (i.e., the magnetic parameters $D$ and $B_{2n}$), e.g., in Fig. 1(c) the solid line for $\Delta_{m,-m} = 0.01$K and the dotted line for $\Delta_{m,-m} = 0$ almost coincide with each other for $T > 3.5$K. With increasing temperature, while $\Gamma_{4,-4}$ decreases rapidly, $\gamma_{m,m'}$ is gradually enhanced. Instead of the QTM mechanism, the spin relaxation becomes a dominant mechanism to decrease $m$, which is reached by opening channels of $|m\rangle \rightarrow |m-1\rangle$. Figure 2(c) shows that the current is determined by the spin relaxation rate $\gamma_{3,4}$ from state $|4\rangle$ to $|3\rangle$. The current for $S = 1$ at higher temperatures (or $\gamma_{m,m'} \gg W_{m,m'}, \Gamma_{m,-m}$) is given by

$$\frac{1}{I_{in}} \approx \frac{1}{2e}\left(\frac{1}{\gamma_{0,1}} + \frac{\gamma_{0,-1} + \gamma_{-1,0} + \gamma_{1,0}}{\gamma_{0,1}W_{1,0} + \gamma_{-1,0}W_{0,-1}}\right), \tag{12}$$

which is difficult to be described simply in the resistance picture as done in Fig. 1(b) and Fig. 2(b). Even so, it is evident that $\gamma_{0,1}$ plays a determinative role in the current generation; $I_{in}$ will be vanishing if $\gamma_{0,1} = 0$. This is greatly different from the unpolarized current in Eq. (10). One can recall that $\gamma_{m,m'}$ affects $I_{in}$ by changing $\rho_m$ of SMM states. Such an indirect effect is usually weak and difficult to be detected in transport measurements[25]. Interestingly, Eq. (12) establishes a decisive relation between the spin relaxation and the inelastic current. It is expected that this result can provide a means to evaluate the transport-induced spin relaxation rate in the SP-STM configuration.

At 1.2K$< T < 3.5$K, the deep dip of $I_{in}$ [solid line in Fig. 1(c)] is as a consequence of competitions between $\Gamma_{m,-m}$ and $\gamma_{m,m'}$, which have opposite temperature dependence. It is a crossover regime of the QTM mechanism and the spin relaxation mechanism.

To further understand the mechanisms of the QTM and the spin relaxation and to distinguish them from each other, we calculate the shot noise spectrum, $S(\omega) = 2 \int_{-\infty}^{\infty} dt e^{i\omega t} [\langle I(t)I(0) \rangle - \langle I \rangle^2]$, employing the widely applied combination-generation approach[34–37]. The Fano factor $F = S(0)/(2eI)$ vs $T$ is plotted in Fig. 2(d), where the corresponding current (dashed line) is indicated for reference. Here $F > 1$ exhibits a super-Poissonian statistics for the QTM process. This bunching effect associated with the QTM is similar to the dynamic spin blockade in Refs.[36,37], where the tunneling of spin minorities (slow channel) modulates the tunneling of spin majorities (fast channel). In the present case, even though there is only one spin channel, the tunneling electrons can still be modulated by the QTM process. When the SMM state is saturated to be $|4\rangle$ by the spin-up electron tunneling, the molecule spin acts on the electrons via spin blockade effect so as to in turn hamper the electron tunneling. For the electron subsystem, it is a longer time waiting during the SMM magnetization tunneling from state $|4\rangle$ to $|-4\rangle$, since time $1/\Gamma_{4,-4} \gg 1/W_{m,m'}$. However, once this slow process is finished, a number of electrons flow through the SMM within a shorter time interval, giving rise to the bunching effect of electrons. For the molecule subsystem, it is manifested by the consecutive transitions $|-4\rangle \rightarrow |-3\rangle ... \rightarrow |4\rangle$. Unlike the QTM mechanism, the spin relaxation processes at higher temperatures are accompanied by a Poissonian behavior of $F = 1$, which is a consequence of stochastic thermal excitations. In the crossover regime, there exhibits a significant super-Poissonian peak, which arises from the competition of $\Gamma_{4,-4}$ and $\gamma_{3,4}$ with comparable magnitude.

Finally, we want to address the elastic current, given by

$$I_{el} = \frac{\pi e^2 V}{2\hbar} \left[ (J_d^2 + J_{ts}^2 \langle S_z^2 \rangle) \left( D_\uparrow^t D_\uparrow^s + D_\downarrow^t D_\downarrow^s \right) + 2 J_d J_{ts} \langle S_z \rangle \left( D_\uparrow^t D_\uparrow^s - D_\downarrow^t D_\downarrow^s \right) \right], \quad (13)$$

with $\langle S_z^2 \rangle = \Sigma_m m^2 \rho_m$ and $\langle S_z \rangle = \Sigma_m m \rho_m$. For large bias under consideration, its introduction provides only a current background, but does not change the above results qualitatively. This current can be significantly suppressed if the setup is made either with $J_d \rightarrow 0$ or with the oppositely polarized tip and substrate. In the latter, the inelastic component is determined by $D_\uparrow^\eta D_\downarrow^{\eta'}$, but the elastic component by $D_\uparrow^\eta D_\uparrow^{\eta'}$. This spin-conserving transport turns to be stochastic processes, obeying the Poissonian statistics.

## IV. SUMMARY

In summary, we theoretically study the fingerprint of QTM of nanomagnets in the nonequilibrium transport measurement by employing a STM with a spin-polarized tip. We find that for a high-polarized tip, the QTM plays a decisive role in the low-temperature inelastic current and thus we can observe the QTM dynamics unambiguously, from which the tunnel splitting can be directly determined. At higher temperatures, we find that the same configuration can be applied to evaluate the transport-induced spin relaxation rate. The same results can be easily obtained for the STM geometry with full polarized substrate. These results might provide an approach to extract the unknown magnetic parameters of the SMMs even though in the absence of the applied magnetic field. To provide more transparent physics, we analytical analyze the case of $S = 1$. We further monitor the current noise spectroscopy, which is of super-Poissonian type for the QTM process but is of Poissonian type for the thermally-excited spin relaxation. This distinct behavior gives an another manner to distinguish the two types of different nonequilibrium dynamics mechanisms.

## V. ACKNOWLEDGMENTS

[1] L. Bogani, W. Wernsdorfer, Nat. mater. **7**, 179 (2008).

[2] A. Cornia, A.C. Fabretti, M. Pacchioni, L. Zobbi, D. Bonacchi, A. Caneschi, D. Gatteschi, R. Biagi, U. Del Pennino, V. De Renzi, L. Gurevich, H.S.J. Van der Zant, Angewandte Chemie Int. Ed. **42**, 1645 (2003).

[3] S. Voss, O. Zander, M. Fonin, and U. Rüdiger, Phys. Rev. B **78**, 155403 (2008).

[4] R.Q. Wang, L. Sheng, R. Shen, B.G. Wang, D.Y. Xing, Phys. Rev. Lett. **105**, 057202 (2010).

[5] H. B. Heersche, Z. de Groot, J.A. Folk, H.S.J. van der Zant, C. Romeike, M.R. Wegewijs, L. Zobbi, D. Barreca, E. Tondello, A. Cornia, Phys. Rev. Lett. **96**, 206801 (2006).

[6] M. H. Jo, J.E. Grose, K. Baheti, M. M. Deshmukh, J.J. Sokol, E.M. Rumberger, D.N. Hendrickson, J.R. Long, H.K. Park, D.C. Ralph, Nano Lett. **6**, 2014 (2006).

[7] A.S. Zyazin, J.W.G. van den Berg, E.A. Osorio, H.S.J. Van der Zant, N.P. Konstantinidis, M. Leijnse, M.R. Wegewijs, F. May, W. Hofstetter, C. Danieli, A. Cornia, Nano Lett. **10**, 3307 (2010).

[8] W. Wernsdorfer, R. Sessoli, Science **284**, 133 (1999).

[9] W. Wernsdorfer, R. Sessoli, A. Caneschi, D. Gatteschi, A. Cornia, Europhys. Lett. **50**, 552 (2000).

[10] A. Nait Abdi, J.P. Bucher, P. Rabu, O. Toulemonde1, M. Drillon, and Ph. Gerbier, J. Appl. Phys. **95**, 7345 (2004).

[11] C. Romeike, M.R. Wegewijs, W. Hofstetter, H. Schoeller, Phys. Rev. Lett. **96**, 196601 (2006); **97**, 206601 (2006).

[12] R.Q. Wang, D.Y. Xing, Phy. Rev B **79**, 193406 (2009).

[13] A.F. Otte, M. Ternes, K. von Bergmann, S. Loth, H. Brune, C.P. Lutz, C.F. Hirjibehedin, A.J. Heinrich, Nat. Phys. **4**, 847 (2008).

[14] J.J. Parks, A.R. Champagne, T.A. Costi, W.W. Shum, A.N. Pasupathy, E. Neuscamman, S. Flores-Torres, P.S. Cornaglia, A.A. Aligia, C.A. Balseiro, G.K.L. Chan, H.D. Abruna, D.C. Ralph, Science **328**, 1370 (2010).

[15] C. Romeike, R. M. Wegewijs, H. Schoeller, Phys. Rev. Lett. **96**, 196805 (2006).

[16] G. González, M.N. Leuenberger, Phys. Rev. Lett. **98**, 256804 (2007).

[17] N. Domingo, E. Bellido, D. Ruiz-Molina, Chem. Soc. Rev. **41**, 258 (2012).

[18] A.J. Heinrich, J.A. Gupta, C.P. Lutz, D.M. Eigler, Science **306**, 466 (2004).

[19] C.F. Hirjibehedin, C.Y. Lin, A.F. Otte, M. Ternes, C.P. Lutz, B.A. Jones, A.J. Heinrich, Science **317**, 1199 (2007).

[20] F. Delgado, J. Fernández-Rossier, Phys. Rev. Lett. **107**, 076804 (2011).

[21] G.H. Kim, T.S. Kim, Phys. Rev. Lett. **92**, 137203 (2004).

[22] F. Meier, L.H. Zhou, J. Wiebe, R. Wiesendanger, Science **320**, 82 (2008).

[23] S. Loth, K. von Bergmann, M. Ternes, A.F. Otte, C.P. Lutz, A.J. Heinrich, Nat. Phys. **6**, 340 (2010).

[24] J. Fransson, O. Eriksson, A.V. Balatsky, Phys. Rev. B **81**, 115454 (2010).

[25] F. Delgado, J.J. Palacios, J. Fernández-Rossier, Phys. Rev. Lett. **104**, 026601 (2010).

[26] S. Krause, L. Berbil-Bautista, G. Herzog, M. Bode, R. Wiesendanger, Science **317**, 1537 (2007).

[27] K. Tao, V.S. Stepanyuk, W. Hergert, I. Rungger, S. Sanvito, P. Bruno, Phys. Rev. Lett. **103**, 057202 (2009).

[28] S. Krause, G. Herzog, A. Schlenhoff, A. Sonntag, R. Wiesendanger, Phys. Rev. Lett. **107**, 186601 (2011).

[29] I. Weymann, J. Barnaś, J. König, J. Martinek, G. Schön, Phys. Rev. B **72**, 113301 (2005).

[30] M. Misiorny, J. Barnaś, Phys. Rev. B **75**, 134425 (2007).

[31] M.N. Leuenberger, D. Loss, Phys. Rev. B **61**, 1286 (2000).

[32] E. Rastelli, A. Tassi, Phys. Rev. B **64**, 064410 (2001); **65**, 092413 (2002).

[33] A. Sieber, et al. Inorg. Chem. **44**, 4315 (2005).

[34] S. Hershfield, J.H. Davies, P. Hyldgaard, C.J. Stanton, J.W. Wilkins, Phys. Rev. B **47**, 1967 (1993).

[35] I. Djuric, B. Dong, H.L. Cui, IEEE Trans. NanoTechnol. **4**, 71 (2005).

[36] A. Cottet, W. Belzig, C. Bruder, Phys. Rev. Lett. **92**, 206801 (2004).

[37] R.Q. Wang, L. Sheng, L.B. Hu, B.G. Wang, D.Y. Xing, Phys. Rev. B **84**, 115304 (2011).

FIG. 1: (Color online) Inelastic current $I_{in}$ in unit of $I_0 = \pi e^2 D_0^t D_0^s / 8\hbar$ as a function (a) of $\Delta_{4,-4}$ and (c) of temperature $T$. (b) Schematic view of spin transitions of $S = 1$ nanomagnet due to the exchanged coupling with unpolarized conduction electrons. The other parameters are $J_{ss} = 0.002$K, $J_{tt} = 0.3$K, $J_{ts} = \sqrt{J_{tt}J_{ss}}$ and $\chi_s = 0$.

FIG. 2: (Color online) $I_{in}/I_0$ as a function (a) of $\Delta_{4,-4}$ and (c) of $\gamma_{3,4}$. (b) Schematic view of spin transitions of $S = 1$ nanomagnet due to exchanged coupling with fully polarized conduction electrons. (d) Variations of Fano factor (solid line) and corresponding current (dashed line) with $T$; $F = 1$ for horizontal dotted line. The other parameters are the same in Fig. 1
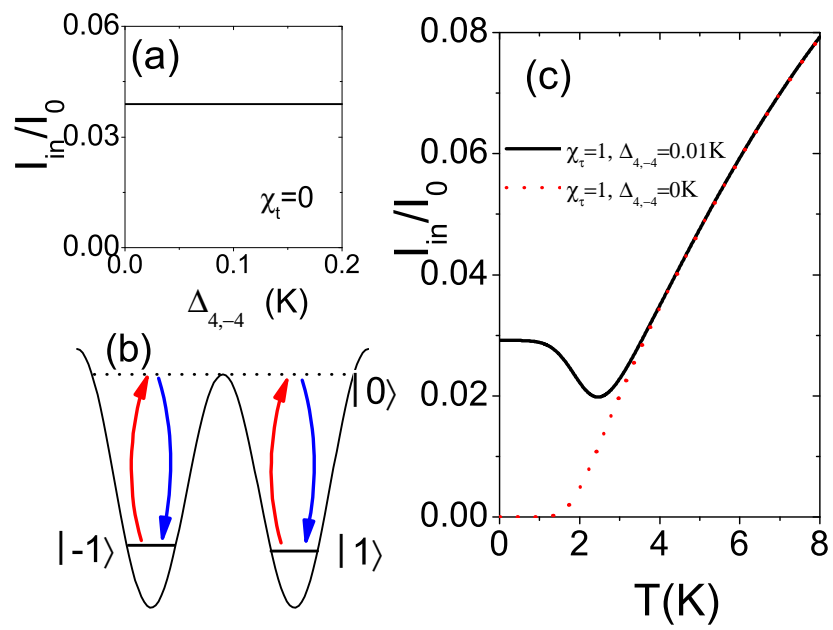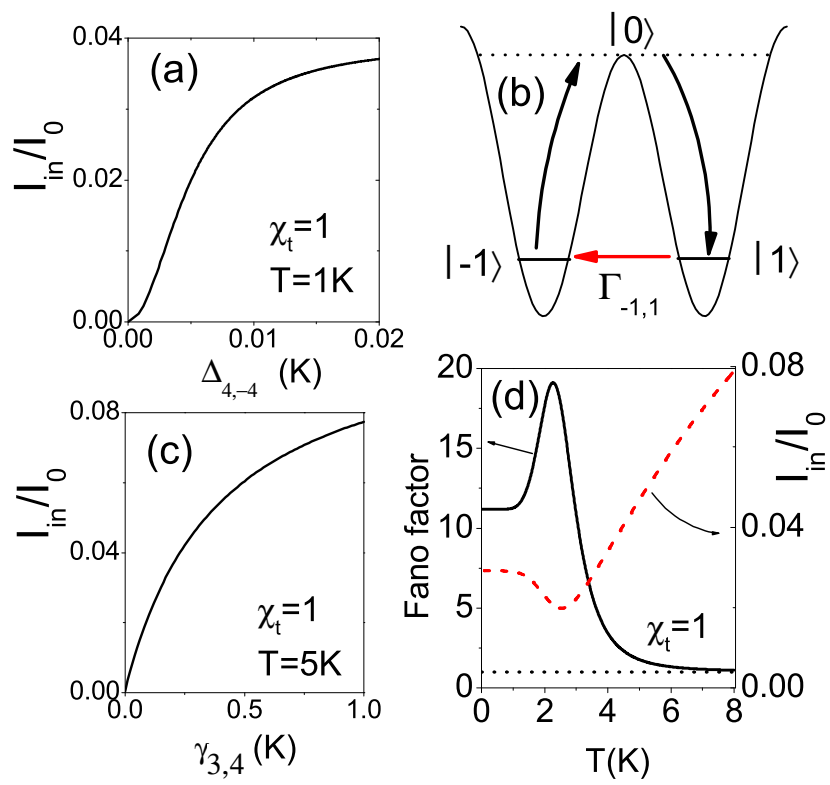
Figure 1    LN13094B    30Mar2012

Figure 2        LN13094B        30Mar2012